Science Advances
AAAS

advances.sciencemag.org/cgi/content/full/5/10/eaaw6670/DC1

Supplementary Materials for

Range of motion in the avian wing is strongly associated with flight behavior and body mass

V. B. Baliga, I. Szabo, D. L. Altshuler*

*Corresponding author. Email: doug@zoology.ubc.ca

Published 23 October 2019, *Sci. Adv.* **5**, eaaw6670 (2019)
DOI: 10.1126/sciadv.aaw6670

The PDF file includes:

Other Supplementary Material for this manuscript includes the following:

(available at advances.sciencemag.org/cgi/content/full/5/10/eaaw6670/DC1)

Data S4 (.tre format). Bayesian maximum clade credibility tree.
Data S5 (Microsoft Excel format). Flight behavior matrix.

Supplementary Materials

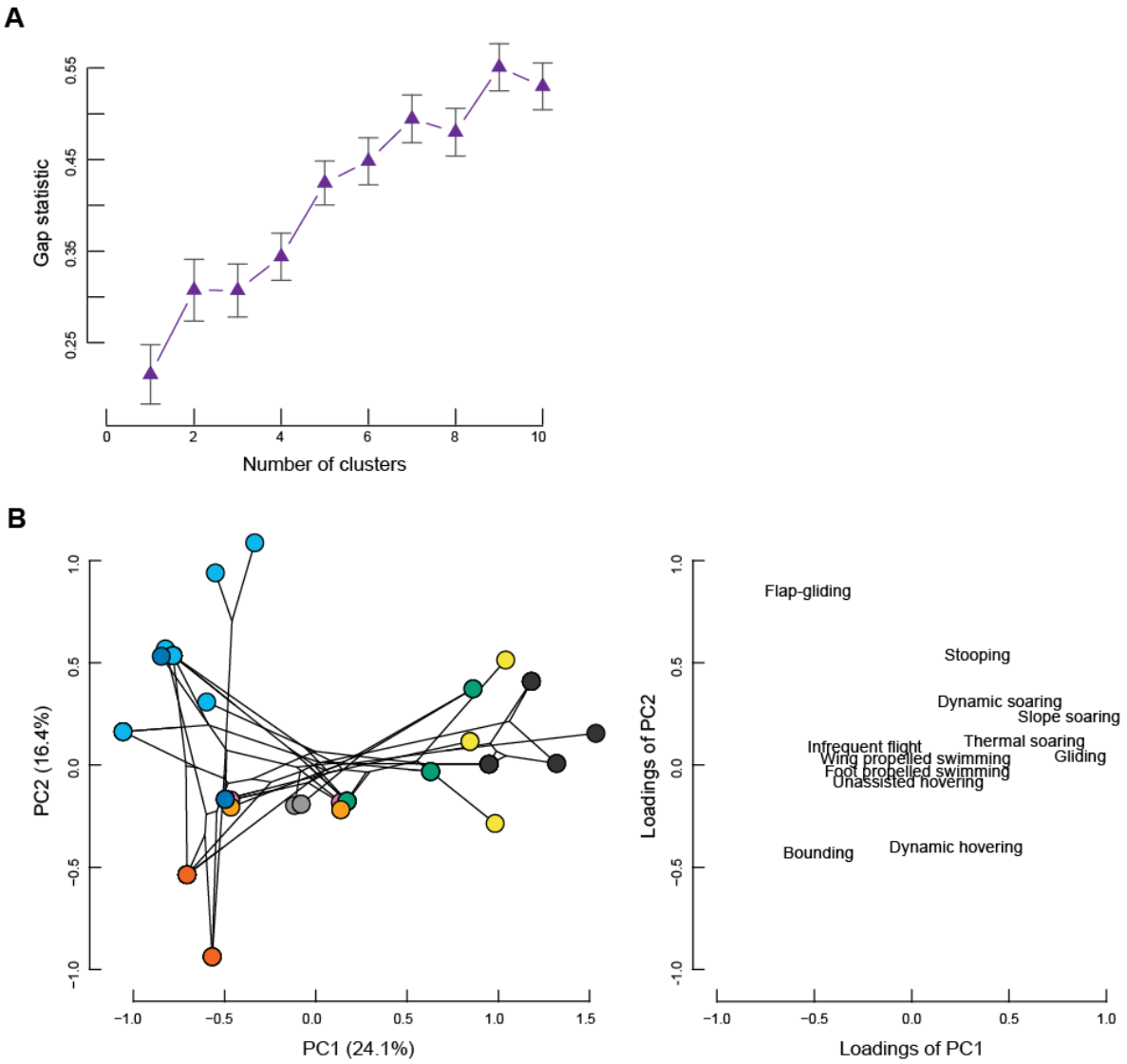

Fig. S1. Determination of number of flight behavior groups. (**A**) Using the gap statistic (*10*), we determined that the 61 species' flight behaviors could be clustered into 9 groups. (**B**) Groups were thereafter named by first applying phylogenetic PCA (*13*) to the flight behavior matrix and using the loading matrix to determine how specific behaviors corresponded to species' ordination. Plotted here are the first two PCs (left) and a plot of variable loadings (right). The behavior that best corresponded with a flight group's position in the PCA was used to name the group. In B, colors match those shown for flight behavior groups in Figs. 1-4 of the main text.

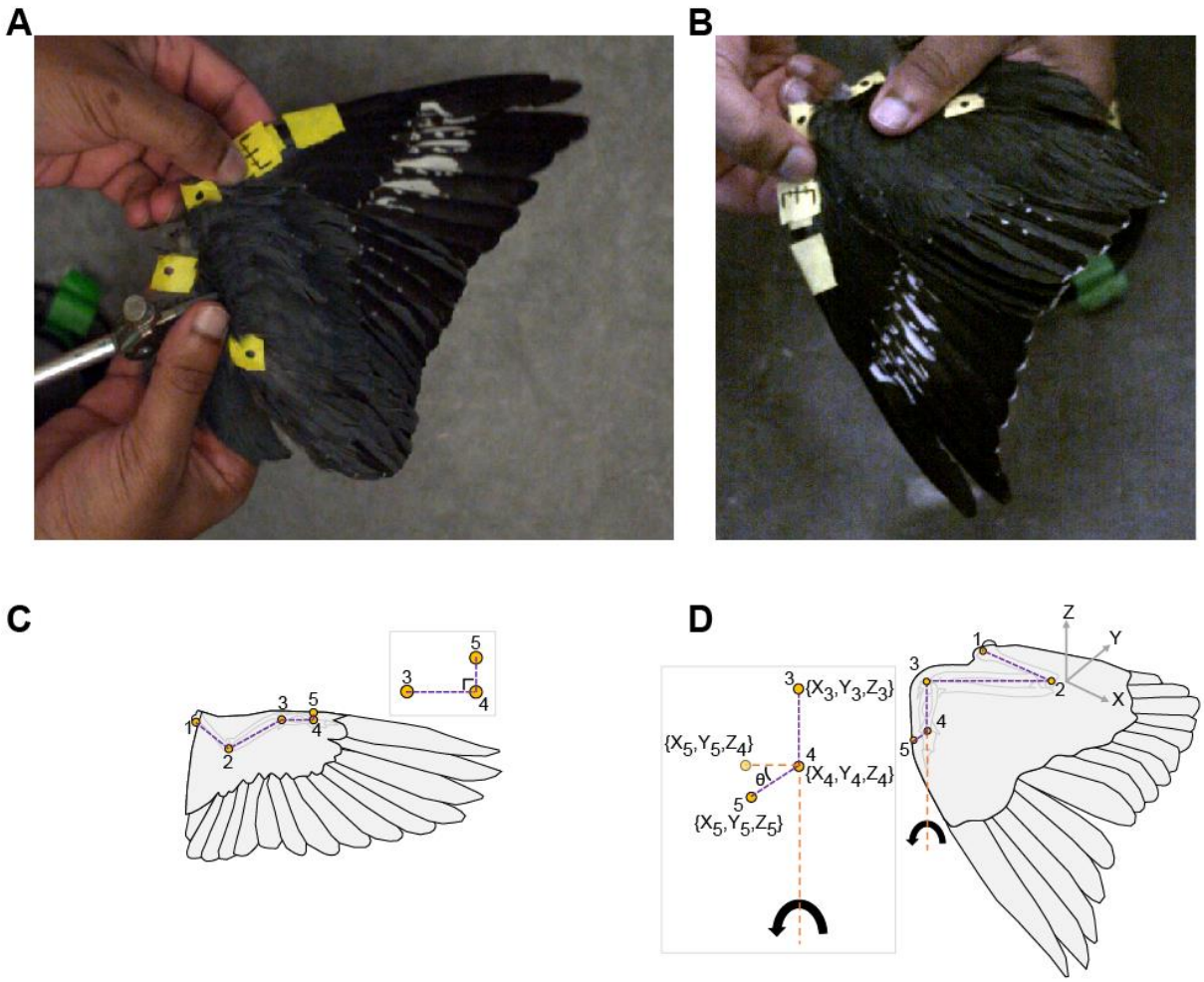

Fig. S2. Placement of markers for capture of ROM from videography. Frames from videos in which (**A**) the extension ROM and (**B**) the bending and twisting capacity was determined for the belted kingfisher (*Megaceryle alcyon*). All points were digitized in 3D. (**C**) Illustration depicting the five markers that were placed on the wing. Inset shows how the position of point 5 is perpendicular to the carpometacarpus (the line connecting points 3 and 4). (**D**) Illustration of the same five markers used to capture bending or twisting. In the inset: pronation of the carpometacarpus was determined by calculating θ. Photo by Vikram B. Baliga.

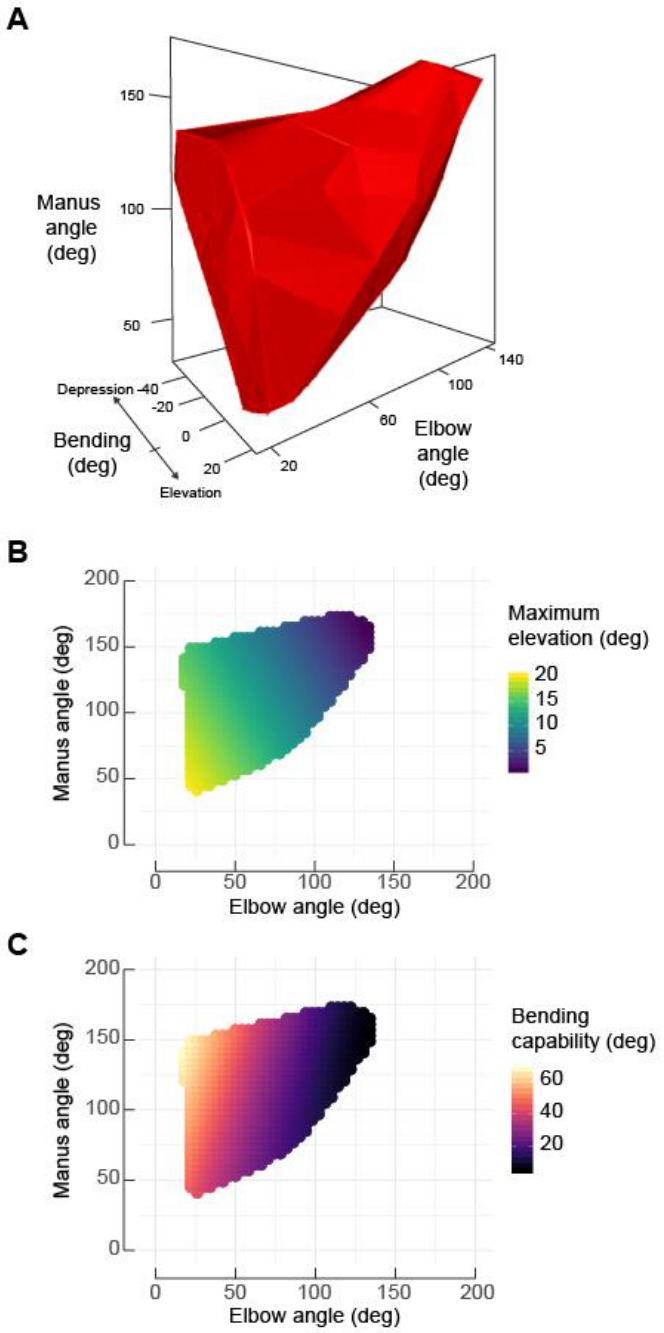

Fig. S3. Determination of out-of-plane motion from angular data. (**A**) To determine bending capability in the wing, manus angle (z-axis), elbow angle (diagonal right), and bending (elevation or depression of the hand wing; diagonal left) were first plotted against each other (here: data from the mallard, *Anas platyrhynchos*). An alpha hull (red shape) was then fit to the 3D shape encapsulating the space occupied by these points. The vertices of this hull were then split into elevation (if they had positive values on the "bending" axis) or depression (negative). (**B**) A regularized neural network was fit to the elevation data to determine maximum elevation capability across extension ROM. (**C**) After using a similar procedure for depression data, neural network outputs for elevation and depression were combined to determine bending capability across extension ROM.

Table S1. Fossil and biogeographic information used for divergence time estimation in BEAST.

MRCA	Fossil name (if applicable)	Age (MYA)	Prior (5-95% dist., MYA) (Distribution)	Original Source
ROOT (all Aves)		66 (minimum)	66.1 – 185 (Lognormal)	*66*
Stem Pici (all Piciformes except Bucconidae and Galbulidae)	*Rupelramphastoides knopfi*	28.3 (fossil) 88.38 – 110 (clade) 40.0 (sampling of taxa)	31.8 – 48.2 (Normal)	*67, 68*
Stem Psittaciformes	*Pulchrapollia gracilis*	53.5 (clade) 39.0 (sampling of taxa)	30.8 – 47.2 (Normal)	*69*
Stem Gruoidea (Aramidae + Psophiidae + Gruidae)	*Parvigrus pohli*	28.3 (minimum)	21.6 – 38.4 (Normal)	*70*
Stem Apodidae	*Scaniacypselus wardi*	47.5 (minimum)	31.8 – 48.2 (Normal)	*71-75*
Stem Phalacrocoracidae	*Oligocrax stoeffelensis*	24.52 (fossil)	6.95 – 25.0 (Normal)	*76*
Stem Galliformes	*Gallinuloides wyomingensis*	51.58 (fossil)	43.6 – 60.0 (Normal)	*77*
Stem Apodiformes	*Eocypselus rowei*	51.58 (fossil)	46.6 – 56.5 (Normal)	*77*
Stem Anatidae		66 (clade) 25 (sampling of taxa)	18.4 – 31.6 (Normal)	*78*
Crown Charadriiformes		55.8	46.8 – 64.8 (Normal)	*79, 80*

We placed parametric prior distributions on the MRCA of lineages as specified by the Prior column, using the topology of our maximum likelihood tree.

Table S2. Comparisons of Bayesian generalized linear mixed models.

Analysis	Formula	DIC	Conditional R^2	Training MSE	Test MSE
Static wing shape	**~ 1**	**-1391.8**	**0.80**	**4.96E-07**	**1.54E-06**
	~ M	-1385.8	0.79	5.06E-07	1.57E-06
	~ F	-1378.9	0.78	5.82E-07	2.01E-06
	~ F+M	-1377.5	0.77	6.10E-07	2.68E-06
	~ F*M	-1362.5	0.77	6.00E-07	9.28E-06
Extension ROM shape	~ 1	-1121.9	0.84	5.17E-06	2.86E-05
	~ M	-1123.7	0.84	5.47E-06	2.94E-05
	~ F	-1124.7	0.84	6.58E-06	3.15E-05
	~ F+M	**-1136.7**	**0.85**	**5.96E-06**	**2.36E-05**
	~ F*M	-1114.7	0.82	5.89E-06	4.44E-05
Linkage trajectory	$\sim A_E$	-7927.5	0.92	0.0133	0.0269
	$\sim A_E + M$	-7927.6	0.92	0.0133	0.0277
	$\sim A_E + F$	-7928.1	0.91	0.0133	0.0194
	$\sim A_E + M + F$	-7927.8	0.91	0.0133	0.0200
	$\sim A_E + M + F + M{:}\,A_E$	-7986.7	0.91	0.0131	0.0213
	$\sim \boldsymbol{A_E + F + F{:}\,A_E}$	**-10038.7**	**0.95**	**0.0101**	**0.0170**
	$\sim A_E + M + F + F{:}\,A_E$	-9767.4	0.94	0.0101	0.0190
	$\sim A_E + M + F + M{:}\,A_E + F{:}\,A_E$	-9799.8	0.94	0.0100	0.0230
Wing aspect ratio	$\sim \boldsymbol{A_M}$	**-3661.7**	**0.94**	**0.0306**	**0.0464**
	$\sim A_M + M$	-3429.4	0.93	0.0306	0.0463
	$\sim A_M + F$	-3429.1	0.94	0.0307	0.0468
	$\sim A_M + M + F$	-3429.1	0.94	0.0307	0.0465
	$\sim A_M + M + F + M{:}\,A_M$	-3467.2	0.94	0.0305	0.0828
	$\sim A_M + F + F{:}\,A_M$	-4166.2	0.95	0.0268	0.0596
	$\sim A_M + M + F + F{:}\,A_M$	-4166.4	0.95	0.0267	0.0613
	$\sim A_M + M + F + M{:}\,A_M + F{:}\,A_M$	-4192.5	0.95	0.0267	0.0610
Bending capability	$\sim S$	268.67	0.90	71.19	55.39
	$\sim \boldsymbol{S + M}$	**264.76**	**0.93**	**61.85**	**51.70**
	$\sim S + F$	268.62	0.93	60.83	55.12
	$\sim S + M + F$	271.74	0.93	58.41	551.14
Twisting capability	$\sim S$	331.27	0.78	286.56	277.58
	$\sim \boldsymbol{S + M}$	**327.76**	**0.82**	**280.61**	**248.36**
	$\sim S + F$	330.64	0.82	274.54	311.80
	$\sim S + M + F$	330.53	0.83	264.99	1500.09

Rows are bolded for models that best fit the data according to Deviance Information Criteria (DIC) and/or Test Mean Squared Error (MSE); see Materials and Methods for details of model formulas. Only in the case of models fit to wing aspect ratio did we find disagreement between the best-fitting model identified by DIC vs. Test MSE. Conditional R^2 was computed (*54*) but not used for model selection.

Table S3. Descriptions of best-fitting Bayesian generalized linear mixed models.

Analysis	Formula	Effect	Coefficient	l-95% CI	u-95% CI	Pagel's λ
Static wing shape	~ 1	intercept	5.70e-05	-2.05e-03	2.16e-03	0.63
Extension ROM shape	$\sim F + M$	$F_{G\&S}$	4.88e-03	-5.12e-03	1.49e-02	0.63
		F_{FPS}	3.08e-03	-7.89e-03	1.37e-02	
		$F_{F\&G}$	1.03e-02	2.81e-03	1.80e-02	
		$F_{F\&SS}$	9.45e-03	8.01e-04	1.87e-02	
		F_{DS}	5.45e-03	-4.01e-03	1.59e-02	
		F_{UH}	5.11e-03	-3.87e-03	1.39e-02	
		$F_{F\&B}$	5.84e-03	-2.68e-03	1.39e-02	
		F_{WPS}	7.32e-03	1.33e-03	1.66e-02	
		F_{IF}	-2.36e-03	-1.30e-02	8.49e-03	
		M	-1.24e-03	-2.46e-03	-3.16e-05	
Linkage trajectory	$\sim A_E + F + F{:}A_E$	A_E	0.70	0.69	0.71	0.86
		$F_{G\&S}$	1.42	1.13	1.67	
		F_{FPS}	2.59	2.31	2.88	
		$F_{F\&G}$	2.39	2.12	2.67	
		$F_{F\&SS}$	2.45	2.21	2.69	
		F_{DS}	0.09	-0.26	0.45	
		F_{UH}	1.60	1.20	1.98	
		$F_{F\&B}$	2.21	1.91	2.51	
		F_{WPS}	2.84	2.54	3.11	
		F_{IF}	2.13	1.73	2.52	
		$A_E{:}F_{FPS}$	-0.23	-0.24	-0.21	
		$A_E{:}F_{F\&G}$	-0.19	-0.21	-0.17	
		$A_E{:}F_{F\&SS}$	-0.17	-0.18	-0.15	
		$A_E{:}F_{DS}$	0.28	0.25	0.32	
		$A_E{:}F_{UH}$	-0.01	-0.04	0.02	
		$A_E{:}F_{F\&B}$	-0.15	-0.17	-0.12	
		$A_E{:}F_{WPS}$	-0.26	-0.28	-0.25	
		$A_E{:}F_{IF}$	-0.13	-0.15	-0.11	
Aspect ratio	$\sim A_M$	intercept	-6.85	-7.16	-6.54	0.80
		A_M	1.70	1.68	1.70	
Bending capability	$\sim S + M$	M	-3.07	-5.00	-1.25	0.03
		S_m	78.50	67.66	89.07	
		S_x	32.74	21.66	43.18	
Twisting capability	$\sim S + M$	M	-5.33	-9.88	-1.11	0.05
		S_m	118.86	92.67	144.71	
		S_x	64.10	38.77	90.96	

For each data set, the formula for the best-fitting Bayesian generalized linear mixed model is indicated under the Formula heading. Coefficients for each fixed effect are presented along with lower (l-95% CI) and upper (u-95% CI) 95% credible intervals. The final column indicates Pagel's λ for the fitted random (phylogenetic) effect. Abbreviations: F, flight behavior group, subscripts according to flight groups' initials; M, natural log-transformed body mass; A_E, natural log-transformed elbow angle; A_M, natural log-transformed manus angle; S, state (a categorization of value at full extension vs. maximum value); S_m, maximum value; S_m, value at full extension.

Table S4. Distributions of effect sizes in mixed models as phylogeny varies.

Analysis	Effect	5th	50th	95th
Static wing shape	Flight behavior group	-0.05	-0.03	-0.01
	Body mass	0	0.01	0.02
Extension ROM shape	Flight behavior group	0.09	0.13	0.19
	Body mass	0.04	0.09	0.11
Linkage trajectory	Flight behavior group	-0.02	0	0.02
	Body mass	0.33	0.35	0.37
Bending capability	Flight behavior group*	-0.04	-0.03	0.01
	Body mass	0.23	0.25	0.27
Twisting capability	Flight behavior group*	0.01	0.02	0.03
	Body mass	0.14	0.18	0.21

Cohen's $f^2$was calculated to determine effect sizes for fixed effects (flight behavior group and body mass). In each analysis phylogenetic sensitivity was determined by recomputing Cohen's f^2 values in Bayesian generalized linear mixed models using the maximum clade credibility tree or one of the 1000 sampled posterior distribution trees. The 5th, 50th, and 95th columns show the corresponding percentile values across the distributions of Cohen's f^2 values, which are also depicted in Fig. 5 (see main text). Asterisks indicate analyses were restricted to four well-represented flight behavior groups.

Table S5. Distributions of phylogenetic signal.

Trait	J'knife 5th	J'knife 50th	J'knife 95th	Phylo 5th	Phylo 50th	Phylo 95th
Humeral length	1.24	1.28	1.32	1.13	1.26	1.35
Ulnar length	1.15	1.18	1.20	1.03	1.15	1.24
Secondaries count	1.11	1.14	1.18	0.96	1.08	1.23
Carpometacarpal count	1.07	1.10	1.13	0.98	1.08	1.16
Wing shape	0.97	0.99	1.01	0.89	0.97	1.04
Flight behavior	0.94	0.96	0.98	0.87	0.94	1.02
Wing area	0.93	0.96	0.99	0.85	0.94	1.02
Wing aspect ratio	0.93	0.95	0.98	0.87	0.93	1.00
Wing length	0.92	0.95	0.97	0.84	0.92	1.00
Body mass	0.90	0.93	0.98	0.82	0.91	0.99
Primaries count	0.83	0.90	0.94	0.79	0.89	0.98
Max twisting capability	0.81	0.82	0.89	0.77	0.80	0.96
Max bending capability	0.69	0.69	0.70	0.66	0.69	0.77
Linkage trajectory length	0.67	0.68	0.70	0.60	0.67	0.72
Extension ROM shape	0.53	0.55	0.57	0.49	0.53	0.58
Extension ROM area	0.49	0.50	0.53	0.43	0.49	0.54

Phylogenetic signal (Blomberg's κ) was computed for all traits. We performed two sensitivity analyses: one in which data were jackknifed (J'knife), and one in which phylogeny was varied (Phylo). The 5th, 50th, and 95th columns show the corresponding percentile values across each sensitivity analysis' distribution of κ -values.

Movie S1. Sample of video used to determine extension ROM in the belted kingfisher (*Megaceryle alcyon*) from one of the three cameras used. Footage is representative but not exhaustive of all manipulations recorded to capture extension ROM for this specimen.

Movie S2. Sample of video used to determine linkage trajectory in the spruce grouse (*Falcipennis canadensis*). Footage comes from one of three cameras used and is representative but not exhaustive of the manipulation employed to capture linkage trajectory.

Movie S3. Sample of video used to determine bending and twisting capability in the mallard (*Anas platyrhynchos*). Footage comes from one of three cameras used and is not exhaustive of the manipulation used to capture out-of-plane range of motion for this specimen.

Data S1. Static morphological data from specimens. Raw static morphological data (except wing shape) for all specimens in this study. Columns: common names, binomial nomenclature, body masses (grams), ID assigned to specimen (this study), primary and secondary feather counts, bone (humeral, ulnar, carpometacarpal) lengths (millimeters), wing areas at full extension (2D planform, in mm^2), wing lengths at full extension (mm), and wing aspect ratios (based on 2D planform).

Data S2. List of genetic sequences sampled. Accession numbers from GenBank used for tree inference for 220 avian and two outgroup species.

Data S3. Maximum likelihood tree. Maximum likelihood tree resulting from our analyses of 220 avian and two outgroup species in RAxML.

Data S4. Bayesian maximum clade credibility tree. Maximum clade credibility tree from analyses in BEAST of 220 avian and two outgroup species.

Data S5. Flight behavior matrix. Flight behaviors exhibited by focal 61 taxa, with each cell indicating whether a species exhibits a particular behavior (on a "yes/no" basis). See Materials and Methods for descriptions of behaviors. Columns: binomial nomenclature, common name, unassisted hovering, dynamic hovering, bounding, flap-gliding, gliding, thermal soaring, slope soaring, dynamic soaring, stooping, foot-propelled swimming, wing-propelled swimming, infrequent flight.